HHS Public Access

Author manuscript

Behav Genet. Author manuscript; available in PMC 2016 March 14.

Published in final edited form as:

Behav Genet. 2014 September ; 44(5): 498–515. doi:10.1007/s10519-014-9665-7.

Regulation of Motor Function and Behavior by Atypical Chemokine Receptor 1

Erich H. Schneider[1], **Stephen C. Fowler**[2], **Michail S. Lionakis**[1], **Muthulekha Swamydas**[1], **Gibran Holmes**[1], **Vivian Diaz**[3], **Jeeva Munasinghe**[3], **Stephen C. Peiper**[4], **Ji-Liang Gao**[1], and **Philip M. Murphy**[1,*]

[1]Laboratory of Molecular Immunology, National Institute of Allergy and Infectious Diseases (NIAID)/NIH, Bethesda, MD, USA

[2]Department of Pharmacology & Toxicology, University of Kansas, Lawrence, KS, USA

[3]In Vivo NMR Center, National Institute of Neurological Diseases and Stroke (NINDS)/NIH, Bethesda, MD, USA

[4]Institute of Pathology, Anatomy & Cell Biology, Jefferson Medical College, Philadelphia, PA, USA

Abstract

Atypical Chemokine Receptor 1 (ACKR1), previously known as the Duffy Antigen Receptor for Chemokines, stands out among chemokine receptors for its high selective expression on Purkinje cells of the cerebellum, consistent with the ability of ACKR1 ligands to activate Purkinje cells *in vitro*. Nevertheless, evidence for ACKR1 regulation of brain function *in vivo* has been lacking. Here we demonstrate that *Ackr1*$^{-/-}$ mice have markedly impaired balance and ataxia when placed on a rotating rod and increased tremor when injected with harmaline, a drug that induces whole-body tremor by activating Purkinje cells. *Ackr1*$^{-/-}$ mice also exhibited impaired exploratory behavior, increased anxiety-like behavior and frequent episodes of marked hypoactivity under low-stress conditions. The behavioral phenotype of *Ackr1*$^{-/-}$ mice was the opposite of the phenotype occurring in mice with cerebellar degeneration and the defects persisted when Ackr1 was deficient only on non-hematopoietic cells. We conclude that normal motor function and behavior depend in part on negative regulation of Purkinje cell activity by Ackr1.

INTRODUCTION

Atypical Chemokine Receptor 1 (ACKR1) is a new standardized name for the Duffy Antigen Receptor for Chemokines (DARC). A member of the 7-transmembrane (7TM) domain protein superfamily, ACKR1 is able to bind specifically to many pro-inflammatory chemokines; however, unlike typical 7TM proteins (but like other ACKRs), it is unable to

*Correspondence to: Philip M. Murphy, M. D., Bldg 10, Room 11N113, NIH, Bethesda, MD 20892; TEL: 301-496-8616; FAX: 301-402-4369; pmm@nih.gov.

Current addresses: Erich H. Schneider, Ph. D., Institute of Pharmacology, Hannover Medical School, Hannover, Germany; Michail S. Lionakis, M. D., Fungal Pathogenesis Unit, Laboratory of Clinical Infectious Diseases, NIAID/NIH, Bethesda, MD, USA

Conflict of interest: The authors declare that they have no conflict of interests.

signal through heterotrimeric G proteins (1–4). Some ACKRs have been shown to signal through arrestin-dependent pathways, but so far evidence of this is lacking for ACKR1 (5).

Another unusual feature of ACKR1 is that, unlike other chemokine receptors, including other ACKRs, ACKR1 does not appear to be expressed on leukocytes; instead, it is expressed by erythrocytes, endothelial cells of post-capillary venules, and in the brain. On erythrocytes it was first identified as the Duffy Antigen, a polymorphic determinant of ACKR1 that defines the Fy blood group system (6, 7). Erythrocyte ACKR1 is thought to scavenge chemokines, to both shape and buffer chemokine concentration gradients during inflammatory responses (8, 9). In addition, in humans, erythrocyte ACKR1 is exploited for cell entry by *Plasmodium vivax*, a major cause of malaria, and red blood cell selective ACKR1-negative individuals with a mutation in the ACKR1 promoter are protected from this disease (10, 11). On endothelial cells (12), ACKR1 is thought to mediate transcytosis of chemokines for subsequent presentation to blood leukocytes (13).

In human brain, ACKR1 is expressed specifically on cerebellar Purkinje neurons as demonstrated by immunohistochemistry (14, 15). Likewise, in mouse brain, *in situ* hybridization data from the Allen brain atlas (16) and published PCR data (17) show that Ackr1 is expressed at highest levels in the cerebellum, and less so in other brain regions like olfactory bulb, parts of the cortex and hypothalamus (16). Consistent with the expression data, Ackr1-binding chemokines have been reported to activate Purkinje cells *in vitro*. In particular, CCL2 induces Ca^{2+} flux in rat Purkinje neurons (18), and CXCL1 and CXCL8 induce Ca^{2+} transients in mouse cerebellar slices (19). CXCL2, which also binds to Ackr1 (20, 21), seems to modulate neurotransmitter release in rat cerebellum by activating ERK in cerebellar granule cells (22). In addition, rat Purkinje neurons respond to the chemokines CCL2, CCL5 and CCL11 (23), all of which also bind to ACKR1 with high affinity (4). A reasonable hypothesis is that these responses are mediated by cognate G protein-coupled chemokine receptors, but negatively regulated by ACKR1 through its known scavenging function.

Despite these advances, evidence for an actual biological role for ACKR1 in brain *in vivo* has been lacking since its brain expression was discovered in 1994. *Ackr1* $^{-/-}$ mice were tested in several behavioral paradigms and reported to show normal performance (24). In rare cases ACKR1 is also silenced in humans in all tissues, including brain, due to a premature stop codon in the *ACKR1* open reading frame. No behavioral abnormalities, however, were described for these persons (25). Since such patients are rare, however, it is difficult to examine them systematically for neurologic and behavioral abnormalities, and the knockout mouse behavioral analysis was limited in scope. Therefore, we decided to re-investigate whether ACKR1 regulates central nervous system function in mice, using motor challenges (rotarod and Morris water maze) or experimental paradigms for the determination of gait, tremor and anxiety-like- or exploratory behavior (force plate actometer, elevated plus maze).

RESULTS

Ackr1 deficiency impairs balance and motor behavior on the rotarod

In rotarod experiments, the animal is subjected to a vestibulomotor challenge by being placed on a rotating cylinder suspended above a platform. Since deficits in motor coordination or balance, e. g. caused by defects in cerebellar function, result in impaired performance in this test (26–28), and since Ackr1 is highly expressed in cerebellum, we hypothesized that rotarod performance would be impaired in Ackr1-deficient mice.

Consistent with this, in four independent experiments with non-littermates (three trials per mouse and different mice in each experiment), *Ackr1*$^{-/-}$ mice fell off the rotarod 30–40% sooner than *Ackr1*$^{+/+}$ control mice that had been used for backcrossing (Figure 1A and B; $p<0.001$). To exclude effects by background mutations in other genes, we repeated the experiments with littermates of *Ackr1*$^{+/-}$ X *Ackr1*$^{+/-}$ crosses in six independent experiments with six trials per mouse and experiment (two days with three trials per mouse). In each experiment, different mice were used. Analysis of all data for all animals demonstrated that rotarod performance was significantly impaired in *Ackr1*$^{-/-}$ mice on day 1 and in both *Ackr1*$^{+/-}$ and *Ackr1*$^{-/-}$ mice on day 2 (Figure 1C), pointing strongly to *Ackr1* as the gene responsible for this phenotype. This appeared to be related to a slower rate of improvement with repeated trials of *Ackr1*$^{-/-}$ mice compared to *Ackr1*$^{+/+}$ mice, which was particularly evident in trials 4 and 5 on day 2 (Figure 1D). Video analysis showed that *Ackr1*$^{-/-}$ mice exhibited evidence of mild ataxia while on the rotarod (Suppl. movies 1 and 2). In particular, the *Ackr1*$^{-/-}$ mouse is slower in stepping forward and the hind feet are carried lower relative to the rod axis, eventually losing their grip. Mice normally make occasional 180° turns relative to the vertical axis, which requires complex motor coordination. Table 1 shows a trend towards a reduced number of 180° turns in *Ackr1*$^{+/-}$- and *Ackr1*$^{-/-}$ mice as compared to *Ackr1*$^{+/+}$ controls. Since the data were not normally distributed, we performed a nonparametric Kruskal-Wallis analysis, yielding a genotype effect close to significance for day 1 ($p = 0.0594$). A *post-hoc* nonparametric Mann-Whitney *U* test yielded a significant difference between Ackr1$^{+/+}$ and Ackr1$^{+/-}$ mice on day 1 of the rotarod experiment ($p = 0.0237$). This result additionally points to impaired motor coordination of *Ackr1*$^{-/-}$ mice.

Ackr1-deficiency reduces locomotion and promotes anxiety-like behavior on the elevated plus maze

The cerebellum may be involved not only in balance but also in emotional processes and anxiety (29, 30). Therefore, we next tested the performance of *Ackr1*-deficient mice on an elevated plus maze, an apparatus designed to make mice choose between either avoiding a potentially harmful situation that induces anxiety or engaging their natural curiosity in explorative behavior. The apparatus consists of two narrow platforms mounted ~60 cm above the floor that intersect perpendicularly at their centers, forming a plus sign. Both arms of one platform have walls (the ‘closed’ arms or ‘safe’ space), whereas both arms of the other platform lack walls (the ‘open’ arms or ‘risky’ space). The animals are initially placed undisturbed in the center, and their movements are tracked (Figure 2A).

Compared to *Ackr1*$^{+/+}$ mice, the total number of arm entries from the center was significantly lower for both *Ackr1*$^{+/-}$ and *Ackr1*$^{-/-}$ mice (Figure 2B). This was associated with reduced average running speed and reduced percentage of open arm entries for *Ackr1*$^{+/-}$ mice, as well as significantly less time spent in the center for *Ackr1*$^{+/-}$ and *Ackr1*$^{-/-}$ mice (Figure 2C–E). The strongest effect of Ackr1 deficiency, however, was only apparent when full length open arm exploration was analyzed. Unlike wild type mice, both *Ackr1*$^{-/-}$ and *Ackr1*$^{+/-}$ mice rarely explored the full length of the open arms (Suppl. Figure 1). To quantitate this phenotype, we calculated the time spent beyond the midpoint of the open arms, highlighted in red in Figure 2A. Both *Ackr1*$^{+/-}$ and *Ackr1*$^{-/-}$ mice spent significantly less time in the outer half of the open arms than *Ackr1*$^{+/+}$ controls, consistent with heightened anxiety (Figure 2F).

Ackr1-deficiency reduces spontaneous locomotion but induces spontaneous anxiety like-behavior and worsens harmaline-induced cerebellar tremor

We next studied behavior under virtually unstressed conditions, where the mouse can freely explore its environment. We used a force plate actometer, a square platform mounted on highly sensitive force transducers capable of detecting force across the platform surface with a time resolution as high as 0.01 s. Male and female *Ackr1*$^{-/-}$, *Ackr1*$^{+/-}$ and *Ackr1*$^{+/+}$ littermates were monitored in 30 min sessions. Neither the force exerted on the plate during running sequences nor the gait frequency was significantly different in *Ackr1*$^{+/-}$ or *Ackr1*$^{-/-}$ mice compared to *Ackr1*$^{+/+}$ controls (Figure 3A and B). In contrast, wall rear duration was prolonged in both *Ackr1*$^{+/-}$ and *Ackr1*$^{-/-}$ mice (Figure 3C). Ackr1 deficiency was also associated with a significantly reduced percentage of total time spent in the platform center, an indicator of increased anxiety consistent with the elevated plus maze results (Figure 3D).

The actometer also revealed markedly reduced spontaneous locomotor activity in both *Ackr1*$^{+/-}$ ($p = 0.002$) and *Ackr1*$^{-/-}$ mice ($p = 0.005$) (Figure 3E). The difference was apparent at the start of the session and persisted throughout. Nevertheless, wild-type controls appeared to ‘settle down’ more than knockouts during the first 3 minutes, probably because they started at a much higher activity level. The Ackr1-dependent reduction in spontaneous activity was caused mainly by a markedly increased frequency of hypoactive events, defined as movement limited to a radius <15mm for at least 5s (Figure 3F, Suppl. videos 3 and 4).

To determine whether Ackr1 might regulate Purkinje neuron function *in vivo*, we injected mice with 15 mg/kg of harmaline, a drug that specifically stimulates Purkinje neurons and deep cerebellar nuclei via excitation of climbing fibers originating from the inferior olivary nucleus. This results in whole-body tremor, and is used as a model of essential tremor (31). Actometer recordings indicated that Ackr1-deficient mice had increased harmaline tremor intensity (Figure 3G) and frequency (Figure 3H), suggesting that Ackr1 modulates Purkinje neuron function *in vivo*.

Ackr1 deficiency does not affect acquisition learning and visual acuity in the Morris water maze apparatus

We next evaluated *Ackr1*-deficient mice in the Morris water maze apparatus, which tests learning, memory and spatial orientation, involving several brain regions, including

hippocampus and cerebellum (28, 32, 33). The animal is tasked to swim until it finds a submerged, invisible platform; safe harbor provides positive reinforcement promoting learning and memory (34). This test was most useful for establishing that Ackr1 deficiency did not affect visual acuity, which can affect outcome from most behavioral tests, specifically from elevated plus maze, rotarod and the Morris water maze test itself. In particular, all mice were able to see the platform when it was elevated above the water surface in the center of the pool. Under these conditions all mice found the platform within a time span that was comparable with the swimming time on the last day of the acquisition learning phase (data not shown).

Figure 4 summarizes results of three independent water maze experiments. There is high inter-experimental variability for most parameters, so the results of each experiment are also shown in Suppl. Figure 2. The results for the distance swum to reach the platform were the most consistent. In particular, although no differences between *Ackr1*$^{-/-}$ and *Ackr1*$^{+/+}$ mice were observed for this parameter during the acquisition phase in any of the three experiments (Figure 4C, left part; Suppl. Figure 2C, G, K, left part), during reversal learning, *Ackr1*$^{-/-}$ mice showed reduced swimming distance compared to *Ackr1*$^{+/+}$ controls in all three experiments (Figure 4C, right part; $p = 0.023$; Suppl. Figure 2C, G, K, right part). Increased thigmotaxis behavior (tendency to swim near the wall of the tank, a measure of anxiety) was observed in *Ackr1*$^{-/-}$ mice in the reversal learning phase of experiments 1 and 2, but not experiment 3 (Suppl. Figure 2D, H, L) . This reached statistical significance for the summarized data as shown in Figure 4D (right part; $p = 0.04$). Differences in swimming speed and latency to find the platform were only found in experiment 1 (Suppl. Figure 2). Learning the platform location was also tested in probe trials with the platform removed. Except for the first water maze experiment, where acquisition learning was impaired in *Ackr1*$^{-/-}$ mice, all mice clearly preferred the quadrant where the platform had been located before (data not shown).

Behavior is regulated mainly by Ackr1 on non-hematopoietic cells

To determine whether hematopoietic or non-hematopoietic Ackr1, or both, regulate behavior, we generated radiation bone marrow chimeras. Six weeks after transplantation in both sexes, engraftment was ~100% when *Ackr1*$^{-/-}$ bone marrow was transferred into irradiated *Ackr1*$^{+/+}$ recipients (*Ackr1*$^{-/-}$➔*Ackr1*$^{+/+}$), and at least 80 % for the converse transfer (*Ackr1*$^{+/+}$ ➔ *Ackr1*$^{-/-}$) (Figure 5).

Consistent with the results shown in Figure 1 for non-chimeric *Ackr1*$^{+/+}$ and *Ackr1*$^{-/-}$ mice, matched chimeras made by transferring *Ackr1*$^{-/-}$ donor bone marrow to irradiated *Ackr1*$^{-/-}$ recipients (*Ackr1*$^{-/-}$➔*Ackr1*$^{-/-}$) fell off the rotarod much sooner than *Ackr1*$^{+/+}$➔*Ackr1*$^{+/+}$ chimeras (Figure 6). Genotype-mismatched *Ackr1*$^{+/+}$➔*Ackr1*$^{-/-}$ chimeras performed as poorly as *Ackr1*$^{-/-}$ ➔*Ackr1*$^{-/-}$ controls, whereas the reciprocally mismatched *Ackr1*$^{-/-}$➔*Ackr1*$^{+/+}$ chimeras performed as well as *Ackr1*$^{+/+}$➔*Ackr1*$^{+/+}$ controls. Thus, impaired rotarod performance depends on Ackr1 deficiency on non-hematopoietic cells, not hematopoietic cells, consistent with effects of Ackr1 in irradiation-resistant brain cells (Figure 6).

A dependence of effects of Ackr1 on non-hematopoietic cells was also seen in three of the four parameters measured on the elevated plus maze (i.e., average running speed, total number of arm entries, and duration in the center) (Figure 7). The fourth parameter, percentage of open arm entries, was reduced in all chimeras tested as compared to corresponding non-chimeric littermates (compare Figures 2E and 7D, and Suppl. Figure 3), and no significant difference was detected between any of the groups. Unlike *Ackr1*$^{+/+}$ mice (Suppl. Figure 1), the majority of chimeric mice made from *Ackr1*$^{+/+}$ recipients, regardless of the donor bone marrow genotype, did not cross the midline of the open arm, indicating a generally increased state of anxiety, possibly attributable to irradiation (35), making this assay non-informative for this parameter.

In actometer experiments, we observed similar differences in behavior between *Ackr1*$^{-/-}$➔*Ackr1*$^{-/-}$ and *Ackr1*$^{+/+}$➔*Ackr1*$^{+/+}$ chimeras as we had observed between non-chimeric *Ackr1*$^{+/+}$ and *Ackr1*$^{-/-}$ controls for all six unchallenged behavioral parameters measured (compare Figure 3A–F with Figure 8A–F). For two of these (i.e., force range within run and wall rear duration), performance was the same or very similar between *Ackr1*$^{-/-}$➔*Ackr1*$^{-/-}$ and *Ackr1*$^{+/+}$➔*Ackr1*$^{+/+}$ chimeras (Figure 8A, C). Not surprisingly then, genotype-mismatched *Ackr1*$^{+/+}$➔*Ackr1*$^{-/-}$ and *Ackr1*$^{-/-}$➔*Ackr1*$^{+/+}$ chimeras performed similarly in these two parameters to each other and to both matched chimera controls (Figure 8A, C). A relatively large difference in behavior was observed between *Ackr1*$^{-/-}$➔*Ackr1*$^{-/-}$ and *Ackr1*$^{+/+}$➔*Ackr1*$^{+/+}$ chimeras as measured by the other four unchallenged parameters (gait rhythm, % of time spent in center, distance moved, and hypoactive events) (Figure 8 B, D–F). Like the rotarod and elevated plus maze tests, *Ackr1*$^{+/+}$➔*Ackr1*$^{-/-}$ chimeras tended to perform most like *Ackr1*$^{-/-}$ ➔*Ackr1*$^{-/-}$ controls, whereas the reciprocally mismatched *Ackr1*$^{-/-}$➔*Ackr1*$^{+/+}$ chimeras performed most like *Ackr1*$^{+/+}$➔*Ackr1*$^{+/+}$ controls (Figure 8 B, D–F), suggesting that non-hematopoietic Ackr1 is important in regulating these behaviors, whereas hematopoietic Ackr1 is not.

With regard to the two parameters measured on the actometer after harmaline challenge, the intensity and frequency of harmaline-induced tremor, irradiation and bone marrow transfer attenuated both in chimeric mice compared to non-chimeric control mice (compare Figure 3G–H with Figure 8G–H). Nevertheless, tremor intensity was still significantly increased in *Ackr1*$^{-/-}$➔*Ackr1*$^{-/-}$ chimeras compared to *Ackr1*$^{+/+}$➔*Ackr1*$^{+/+}$ chimeras, phenocopying non-chimeric control mice (Figure 8G). *Ackr1*$^{+/+}$➔*Ackr1*$^{-/-}$ and *Ackr1*$^{-/-}$➔*Ackr1*$^{+/+}$ genotype-mismatched chimeras both had a low tremor phenotype similar to *Ackr1*$^{+/+}$➔*Ackr1*$^{+/+}$ chimeras, suggesting that both hematopoietic and non-hematopoietic Ackr1may contribute to this phenotype (Figure 8G).

Ackr1 deficiency does not affect macroscopic brain anatomy

The brain of the *Ackr1* knockout mouse has been reported to be macroscopically normal and there were no histological differences detected (24). However, since behavioral phenotypes had not previously been identified in this mouse, we decided to revisit this question. Using magnetic resonance imaging with brains from non-littermate *Ackr1*$^{+/+}$- and *Ackr1*$^{-/-}$ mice, we observed no difference in cerebellar size between *Ackr1*$^{+/+}$ and *Ackr1*$^{-/-}$ mice, confirming the previous report (24) (Suppl. Figure 4 A, B). A comparison of individual

brain slices across the entire brain also found no difference, except in the dorsal part, where *Ackr1*$^{-/-}$ brain appeared slightly smaller (Suppl. Figure 4C). However, we cannot exclude the possibility that this may be caused by respiration-induced motion artifacts in this region, which contains the brain stem.

DISCUSSION

In this study, we report the first evidence that the atypical chemokine receptor Ackr1 regulates central nervous system function *in vivo*. Combined results from genetic, immunologic and pharmacologic analysis using *Ackr1*$^{-/-}$ mice, radiation chimeric mice, and the tremor-inducing drug harmaline all point to the cerebellum, and in particular Purkinje cells, as the key site of Ackr1 action *in vivo*. This is consistent with previously published results demonstrating selective very high expression of Ackr1 in cerebellum, specifically on Purkinje cells (14–16), which are known to respond to Ackr1 ligands in vitro (4, 18, 19).

Our results disagree with Luo *et al*, who had previously reported that Ackr1 deficiency did not affect performance in 15 different behavior paradigms, including two that we used (water maze and rotarod) (24). This group used an independently derived line of *Ackr1*$^{-/-}$ mice to obtain these negative results, and did not specify the experimental conditions, which could have differed substantially from ours and affected the outcome. Moreover, we used two additional tests, including ‘time spent in the terminal half of the opens arms’ on the elevated plus maze test, which is a highly sensitive measure of anxiety-like behavior, and the actometer, which allows highly sensitive digital analysis of mouse motion. Finally, we verified the phenotypes we discovered using three complementary types of mouse breeding paradigms (backcrossed, littermates and radiation chimeras).

Of the eighteen parameters measured across the four types of apparatus used in our study (one for the rotarod, five for the elevated plus maze, four for the Morris water maze and eight for the actometer), *Ackr1*$^{-/-}$ performance was abnormal (different from *Ackr1*$^{+/+}$) in twelve. Four of the twelve were designed to measure anxiety-like behavior, although not specifically for the cerebellum, and the performances of the knockout mice were consistent with an increase in this behavioral state (restricted exploration of the terminal half of the open arms on the elevated plus maze, increased thigmotaxis in the Morris water maze, and decreased time spent in the center of the actometer and the elevated plus maze). The remaining eight parameters were used to measure locomotor activity and motor coordination in various ways, and the performances of the knockout mice were decreased in all eight. Of these eight, three (time on the rotarod, and harmaline-induced tremor intensity and frequency) are most clearly related to cerebellar function, where Ackr1 is highly expressed.

Impaired rotarod performance was unlikely to be caused by impaired vision, since visual testing of the knockouts in the Morris water maze was normal, or by impaired motor learning, since after the sixth rotarod session *Ackr1*$^{-/-}$ and *Ackr1*$^{+/+}$ mouse performance was the same. Moreover, it is unlikely that muscle weakness was responsible for reduced rotarod performance in Ackr1-deficient animals, because Ackr1$^{+/-}$- and Ackr1$^{-/-}$ mice did not show a significantly reduced force range within run as compared to Ackr1$^{+/+}$ mice (Figure 3A). More likely contributing factors include ataxia, general hypoactivity, and increased anxiety.

Ataxia was directly observed on the rotarod rotarod, which represents a rather complex vestibulomotor challenge, whereas the virtually unchallenging actometer conditions revealed only a non-significant trend towards reduced gait frequency and running force. Hypoactivity was apparent in *Ackr1*$^{-/-}$ mice in five tests not specifically designed to interrogate cerebellar function, three on the actometer (wall rear duration, number of hypoactive events and distance moved) and two on the the elevated plus maze (running speed and total number of arm entries), and has previously been discussed as an explanation for poor rotarod performance by the R6/2 mouse model of Huntington's disease (36). Increased wall rear duration may indicate impaired response termination, similar to results previously reported for D_2R knockouts that show Parkinson-like symptoms (36, 37). However, wall rear duration is also used as a measure of non-selective attention in animal models of attention-deficit hyperactivity disorder (38). Defects in both motor systems and cognitive functions could contribute to this phenotype.

The harmaline experiments provide the most direct *in vivo* evidence of Ackr1 action in the cerebellum. Harmaline is a β-carboline alkaloid that specifically stimulates rhythmic firing of neurons in the inferior olive (IO) of the brainstem. Each IO neuron projects onto a Purkinje cell *via* a "climbing fiber". Purkinje neurons in turn connect to neurons of the deep cerebellar nuclei (DCN) that mediate cerebellar output. Some DCN neurons project back to the IO in an inhibitory way, resulting in a closed IO-, Purkinje- and DCN-neuron regulatory loop (39). The DCN represents the only output of the cerebellum and is indispensable for harmaline-induced tremor, projecting the harmaline-induced firing pattern from IO- to cerebellar Purkinje neurons (31). Mice with Purkinje cell degeneration (PCD mice) still express harmaline tremor, but with reduced intensity and frequency compared to wild-type controls (31, 40), suggesting that Purkinje neurons are not required for harmaline tremor (31), but modulate it. Our results obtained with *Ackr1*$^{-/-}$ mice suggest that Ackr1 on Purkinje neurons may alter tremor output from the DCN, probably by modulating Purkinje cell activity. Our results therefore point to an inhibitory effect of Ackr1 on the cerebellar output of harmaline-induced tremor, which will be discussed below.

The six parameters that were not clearly abnormal in *Ackr1*$^{-/-}$ mice include three on the water maze (latency and distance to find the platform, and swimming speed), and two on the actometer that were previously discussed (gait rhythm and force range within run). Due to poor reproducibility, the data from the water maze tests should be interpreted with caution. *Ackr1*$^{-/-}$ mice appeared to perform better than controls in the reversal learning paradigm, as indicated by decreased distance swum to find the platform in the reversal learning phase. Since acquisition learning was not influenced by Ackr1-deficiency, Ackr1 might affect behavioral flexibility and adaptation to new environmental conditions.

A weak gene dosage effect can be seen in the rotarod results (Figure 1) and in some of the actometer data (Figure 3A, D, H), resulting in an intermediate phenotype of *Ackr1*$^{+/-}$ mice as compared to *Ackr1*$^{-/-}$ animals and *Ackr1*$^{+/+}$ controls. In most cases, however, the behavior of *Ackr1*$^{+/-}$ mice was similar to the behavior of full knockouts. Thus, maximum Ackr1 expression is required to reconstitute wild-type behavior.

Bone marrow chimera experiments revealed that most behavioral phenotypes were fully determined by the Ackr1 genotype of the recipient mouse. Thus, we conclude that these phenotypes are due to Ackr1 deficiency on Purkinje cells and possibly neurons from other brain regions. A moderate effect of donor genotype in *Ackr1*$^{+/+}$➔*Ackr1*$^{-/-}$ mice reached significance only for the percentage of time spent in the center and for the number of hypoactive events (actometer, Figure 8 D, F) as well as for average running speed (elevated plus maze, Figure 7A), suggesting a limited contribution of hematopoietic Ackr1. The *Ackr1*$^{-/-}$ ➔ *Ackr1*$^{+/+}$ bone marrow chimeras imitate the situation in malaria-resistant Ackr1-negative humans (11) that selectively lack Ackr1 on red blood cells, while receptor expression is maintained in other tissues, e.g. vascular endothelium (41). No psychological or behavioral abnormalities have been described for these persons, which is consistent with the absence of a behavioral phenotype in our *Ackr1*$^{-/-}$ ➔ *Ackr*$^{+/+}$ bone marrow chimeras.

Importantly, most of the behaviors we found to be abnormal in the *Ackr1*$^{-/-}$ mouse, even anxiety-like behavior, have also been reported to be abnormal in one or more of three well-known mouse models of selective cerebellar degeneration: the Lurcher mouse (Lc/+), the Purkinje cell degeneration mouse (pcd/pcd) and the “nervous” mouse (nr/nr) (Table 2). All three models lose Purkinje neurons almost completely and – depending on the mutation – undergo degeneration of other cerebellar regions and other types of neurons like the granular or molecular layer (28, 30, 42, 43). Thus, it is plausible that *Ackr1* deficiency in cerebellum, and not in other brain regions where it is expressed, accounts for most if not all of the behavioral phenotypes in *Ackr1*$^{-/-}$ mice. However, interestingly, the behavioral phenotypes in these three cerebellar degeneration models are mostly the opposite of the corresponding phenotypes in *Ackr1*$^{-/-}$ mice. Only rotarod performance was impaired in all four mutant mice (28, 44, 45). A reasonable hypothesis to explain these results is that Ackr1 functions on neurons, as it does on erythrocytes, as a negative regulator, so that its loss increases cerebellar function, leading to the opposite phenotype as in the selective cerebellar degeneration mutants. Mechanisms of negative regulation could include scavenging of chemokines that act at G protein-coupled chemokine receptors on neurons, alternative signaling by neuronal Ackr1 in response to cognate chemokines produced by neurons and/or microglial cells, even signaling or scavenging by Ackr1 after binding non-chemokine ligands, including known neurotransmitters. Alternatively, Ackr1 could present chemokines to signaling receptors on neurons. The levels of free chemokines in blood and cerebellum may be governed by a balance of binding to Ackr1, dissociation from Ackr1 and by the rate of chemokine metabolism.

Additional work will be needed to test each of these possibilities. However, there are already reports indicating that pieces of the model are in place and that Ackr1-binding chemokines directly stimulate cerebellar Purkinje neurons, which motivated our work. In particular, Purkinje neurons, in addition to expressing Ackr1, express the Ackr1-binding chemokine CCL2 and its receptor CCR2, as well as receptors for the Ackr1-binding chemokines CCL5 and CCL11 (18, 23, 46); CCL2 has been reported to induce Ca^{2+} flux in isolated rat Purkinje neurons (18); the Ackr1-binding chemokine CXCL8 causes Ca^{2+} transients and enhances neurotransmitter release in mouse cerebellar slices (19); and CXCL2, which also binds to Ackr1 (20), causes ERK activation and modulates neurotransmitter release in rat cerebellum

(22). In addition, brain mast cells are active under basal non-inflammatory conditions (47) and can release chemokines, including the Ackr1 ligands CCL2 and CCL5 (48). Moreover, blockade of central mast cell activation has been reported to be associated with increased anxiety-like behavior in mice (49), indicating another link between behavior and immune function. Astrocytes and microglial cells also express chemokines, including Ackr1 ligands (50). Another level of potential complexity is added by the ability of Ackr1 to influence signaling of other chemokine receptors like CCR5 by forming hetero-oligomers (51). It is intriguing to consider that Ackr1 might also interact in a chemokine-dependent manner with neurotransmitter receptors on Purkinje neurons and therefore modulate “classic” neurotransmitter responses.

In summary, our results demonstrate that Ackr1 plays an important role in regulating the central nervous system at the level of motor function and behavior. As indicated by our MRI results, Ackr1 deficiency does not result in gross abnormalities of the cerebellum and other brain regions, but rather seems to affect neurotransmission and activity of Purkinje neurons. In addition to neuropeptides and neurotransmitters, chemokines may in fact represent a “third major system of communication in the brain” (52). To our knowledge, this is the most detailed behavioral characterization available for a chemokine receptor-deficient mouse. Our results provide a starting point for deeper investigation of the role of chemokines in the modulation of cerebellar function and – *via* cerebellar projections – of other brain areas.

Methods

Laboratory animals

Ackr1$^{-/-}$ mice generated as previously described (8) were backcrossed at least 10 generations to C57Bl/6 mice, strain 664 (Jackson Laboratories, Woods Hole, MA) and, unless otherwise indicated, were bred in the same facility. Except for littermates, mice were housed separately by genotype, a maximum of five mice per cage; all mice were maintained at 22°C on a 12-h light/dark cycle (lights off at 6 pm). Mice were transferred to the behavior laboratory at least one week prior to the experiment, and tested between 10 am and 5 pm. Except for radiation chimeras, whose ages were heterogeneous, the groups were age-matched with a maximum difference of two weeks. All experiments complied with guidelines set by the NIAID Animal Care and Use Committee (NIH).

Rotarod Experiments

Three to five month old mice were tested on one- or five-station rotarods (MedAssociates, St. Albans, VT, USA) from 12-6 pm. Each experiment involved two training sessions and 1–2 test sessions. Training session 1 consisted of a habituation trial on a stationary rod and three trials at 4 rpm, each lasting 60 s, with 45 seconds rest in between. 24 h later, training session 2 began, consisting of 3 trials in which the rod accelerated from 4 to 16 rpm within 100 seconds, with 100 seconds rest in between. The test session began 24 hours later, and consisted of three acceleration trials (4 to 40 rpm over 300 seconds) with 5–10 minutes rest in between. The endpoint was defined to occur when the mouse fell off the rotarod and disrupted an infrared beam. If animals started to cling to the rod to rotate passively, specifically at higher rotarod speeds, we did not intervene, but waited for the animals to fall

off the rod. In littermate experiments, the test session was repeated 24 h later with the same animals, but in reversed order to avoid circadian rhythm effects. The frequency of 180° turns made on the rotarod relative to vertical was calculated by dividing the mean number of turns by the mean trial duration for each individual animal and experimental day. All experiments were performed at full illumination. The rotarod was cleaned between trials.

Elevated Plus Maze Experiments

3–4 month old mice were tested once for 5 min on a plus sign-shaped maze with two open and two closed arms situated 60 cm above the floor and illuminated at 60–75 lux in the center. Each arm is 30 cm long and 5 cm wide. The mouse is placed in the center (5 × 5 cm) and allowed to freely explore the maze. Movements were recorded using an Ethovision video-tracking system (Noldus, Wageningen, Netherlands). The maze was cleaned, if necessary, with 70% ethanol. The experiment followed the rotarod experiment during which the mice got habituated to an “out of cage” experience.

Actometer Experiments

Development of the force-plate actometer has been previously described in detail (53). In brief, the actometer consists of a force-sensing plate (42 × 42 cm) mounted on force transducers in the four corners, which establish the location of the center of mass of the animal. The system produces a signal that depends on the weight and movements of the animal exploring the space. An enclosure suspended 2 mm above the surface confines the animal. Mice were placed in the center and allowed to freely explore the plate. Measurements were made for 30 min at an illumination of ~45 lux during the light phase between 10 am and 6 pm at a time resolution of 100 Hz and a force resolution of 0.2 gram-force, and were also recorded using a digital camera. The actometer was cleaned between sessions with 70% ethanol.

Locomotor activity was determined by calculating the distance moved during a session, based on the smoothed force variations (moving average of 9 data points). ‘Hypoactive events’ were defined as movement within a radius of <15 mm for at least 5 s. The percentage of time spent in the center was defined as the time spent in the central square that occupies 6% of the force plate area.

Within run force range and gait rhythm were determined from “long runs”, defined as periods of lateral movements over a distance of 20 cm or more within a time frame of 2 s, following an almost straight line between starting and ending points. Straightness of the trajectory was evaluated by analysis of the obtuse angle of a triangle formed by a straight line connecting starting and ending point and the two segments from starting point to the middle and from ending point to the middle. An obtuse angle of 180° would mean a totally straight line. The run was included in the analysis if the obtuse angle was greater than 160°.

For the determination of wall rear number and duration, the raw data of the force variations were smoothed (moving average of 9 data points), transformed to percent of body weight and the mean (100%) was subtracted. Wall rears were defined as an off-load force between 5% and 40%, lasting at least 0.25 s. This discriminates wall rears from jumps (maximum

off-load force 100%) and locomotion (off-load force between 30% and 90%, but shorter duration than 0.25 s).

Harmaline-induced tremor was investigated using ~5 month old *Ackr1*$^{-/-}$ and *Ackr1*$^{+/+}$ littermates. First, PBS buffer was injected (5 ml/kg i.p.) followed immediately by a 30 min actometer session. 10–24 days later, the same animals were injected i.p. with 15 mg/kg harmaline (3 mg/mL in PBS) and again immediately monitored on the actometer for 30 min. Sessions were not performed after 5 pm to avoid any change of behavior from anticipating the dark phase. For the quantitation of harmaline tremor intensity and frequency, the raw data (expressed as percent of body weight with offset removed and after application of the Hanning data window) were converted to power spectra by a Fourier transformation (MatLab). The power spectra were calculated for each 10-s time frame of the recording session. Then the twelve 10-s frames with the highest peak power between 8 and 18 Hz were chosen for each mouse and averaged together, resulting in the maximum tremor exhibited by each individual mouse. This method was used to exclude “silent” periods that occur between bouts of harmaline tremor expression. From the resulting average power spectrum for each individual animal the parameters “peak power” and “frequency at peak” were calculated and subjected to statistical analysis.

For characterization of the mice in the bone marrow transfer experiments, experiments with PBS- and harmaline injection were performed essentially as described above, but observation time was reduced to 20 min, starting at 10 min after PBS- or harmaline injection. Since the maximum of the harmaline tremor is not reached before 10 min post-injection, the shortening of the time does not affect the harmaline tremor data calculated from the peak tremor.

Water Maze Experiments

The water-maze consists of grey PVC and has a diameter of 100 cm and a height of 45 cm. The water is kept at ~22°C and is stained with non-toxic white paint to increase contrast and rendering it opaque. Lights were covered to eliminate reflections. The pool area was illuminated indirectly at 30–40 lux on the water surface. A Perspex platform (9×9 cm), is placed 0.5–0.8 cm below the surface, invisible to the swimming mouse, ~10 cm from the pool edge. Distal visual cues (wall posters ~0.50–0.75 m in size with different geometrical patterns) surround the pool. The experiment consists of four phases. (1) Habituation (day1): Mice are given three swim trials, each 60 s long, with 10–15 min rest in between. (2) Acquisition learning phase (7 consecutive days, 4 trials per day): Mice are released from 4 different symmetrical positions on the pool perimeter and attempt to find the platform, which is kept at the same position. Each trial lasts 60 s with 10–15 min rest in between. If unsuccessful, the mouse is placed on the platform for 10 s to foster learning. After each trial, the mice are dried with a paper towel under a heat lamp. Visual orientation prior to release into the pool is prevented using a non-transparent box to transport mice to the water maze. On the day following the 7-day acquisition phase, a probe trial is performed, during which the platform is removed from the pool and each mouse is placed in the pool for 60 s. (3) Reversal learning phase: the day after the acquisition test, the platform is moved to a different position and kept there for the following 4 days. During this time, the mice are

tested according to the same protocol as described for the acquisition learning phase. Then, the platform is removed for a second probe trial. (4) Visual cue test: immediately after the reversal test, the hidden platform is raised above the water surface in the center of the pool. Two visual cue tests were performed to let the mice find the visible platform. Swim paths were recorded using an Ethovision video-tracking system (Noldus, Wageningen, Netherlands). For the acquisition and reversal phases the variables recorded were latency to reach the platform, mean swimming speed, swim path distance as well as percentage of the total time spent along the edge of the water maze (% thigmotaxis time). For the probe trials, the variables recorded were time to swim to the prior location of the hidden platform (latency), number of crossings (frequency) over the prior location of the hidden platform, time spent in the vicinity (quadrant of the circular pool) where the platform had been located, number of entries into the quadrant where the platform had been located, and mean swim speed.

Magnetic Resonance Imaging (MRI)

All studies complied with the guide for the care and use of Laboratory Animal Resources (1996), National Research Council, and approved by the National Institute of Neurologic Diseases and Stroke (NIH) Animal Care and Use Committee. Mice were anesthetized (1.5% isofluorane), and body core temperature was maintained and monitored at 37°C with a heated circulating water pad. A pressure transducer was positioned to monitor respiration. Mice were then placed in a stereotaxic holder and mounted in a 72 mm volume (transmit)/ 25 mm surface (receive) radio frequency coil ensemble for MRI. The MRI experiments were performed on a horizontal bore 7 Tesla scanner operating on a Bruker Avance platform (Bruker Biospin Inc. Bellerica, MA). Three mutually perpendicular scout images were acquired through the brain to localize the brain. Subsequently, 15 T_2 weighted axial slices (1 mm thick) encompassing the entire brain (*Field-of-view [FOV] = 19.2 × 19.2 mm*, in-plane resolution of 75 mm, echo time [*TE*] = 48 ms, repetition time [TR] = 3000 ms, echo train length = 8 and number of averages [NA] = 20, total imaging time 32 minutes) were acquired using a spin-echo pulse sequence to delineate anatomical details. For data analysis, T_2 weighted images were displayed slice by slice and regions of interests were drawn to calculate the area of the brain using Image J.

Generation of Bone Marrow Chimeras

Recipient mice were γ-irradiated with 900 Rad in the morning and were reconstituted with 5 × 10^6 donor bone marrow cells in 200 μl buffer (isolated during the five hours after irradiation) 6–8h after irradiation via tail vein injection. Recipients then received trimethoprim-sulfamethoxazole in autoclaved water for 4 weeks. Recipient and donor mice were 2–4 months old at the time of bone marrow transfer. Nineteen males (5 *Ackr1*$^{+/+}$ ➔ *Ackr1*$^{+/+}$, 4 *Ackr1*$^{+/+}$ ➔ *Ackr1*$^{-/-}$, 5 *Ackr1*$^{-/-}$ ➔ *Ackr1*$^{+/+}$, 5 *Ackr1*$^{-/-}$ ➔ *Ackr1*$^{-/-}$) and 21 females (5 *Ackr1*$^{+/+}$ ➔ *Ackr1*$^{+/+}$, 6 *Ackr1*$^{+/+}$ ➔ *Ackr1*$^{-/-}$, 5 *Ackr1*$^{-/-}$➔ *Ackr1*$^{+/+}$, 5 *Ackr1*$^{-/-}$➔*Ackr1*$^{-/-}$) were used. Blood genotyping was performed at ~6 weeks after bone marrow reconstitution to assess the extent of engraftment. Rotarod and elevated plus maze experiments with bone marrow chimeras were performed ~8 weeks after reconstitution. Actometer experiments were performed at ~9 weeks (PBS control experiment) or ~13 weeks (harmaline experiment) after reconstitution.

Genotyping

Ear punches were incubated for 2 h at 55°C in 50 μl lysis buffer (100 mM Tris-HCl [pH 8.0], 100 mM NaCl, 10 mM EDTA [pH 8.0], 0.2 % SDS and 0.8 mg/ml proteinase K). Samples were vortexed, diluted with 450 μL of DEPC-treated water, then centrifuged for 6 min at 7500 rpm.

Genotyping was performed with a three primer system:1) SCP440 (5'-GTCTAGCCCTGCACATACC-3'), 2) DARCneo (5'-TATGGCGCGCCATCGATCTC-3') and 3) DuffyCommon (5'-CCAGTAGCCCAGGTTGCATA-3'). 2 μl of ear punch extract were added to 23 μl of Platinum PCR Supermix™ (Life Technologies, Carlsbad, CA) containing 200–500 nM primers and amplified by PCR as follows: 3 min at 94°C, followed by 34 cycles of 30 s at 94°C, 30 s at 60°C, and 35 s at 72°C, followed by 7 min at 72 °C. Wild type and gene-targeted amplicons were 452 and 300 bp, respectively.Genotyping of chimeras was performed from blood drawn ~6 weeks after BMT. DNA was purified from 100 μl of blood (diluted with 100 μl PBS buffer) using the QiaAMP DNA blood mini kit™ (Quiagen, Hilden, Germany). Percentage of engraftment was determined by comparison with calibration samples generated from mixtures of wild-type and *Ackr1*$^{-/-}$ blood containing 0, 20, 40, 60, 80 and 100 % wild-type blood.

Supplementary Material

Refer to Web version on PubMed Central for supplementary material.

Acknowledgments

This work was supported by the Division of Intramural Research, National Institute of Allergy and Infectious Diseases, NIH, USA. Financial support was also provided to E. H. S. through German Research Foundation Grant SCHN 1192/1-1. S.C. Fowler received support from NIH grant HD002528 and from the Life Span Institute at the University of Kansas. Experimental support by Alex Bredenkamp is gratefully acknowledged.

REFERENCES

1. Chaudhuri A, Polyakova J, Zbrzezna V, Williams K, Gulati S, Pogo AO. Cloning of glycoprotein D cDNA, which encodes the major subunit of the Duffy blood group system and the receptor for the Plasmodium vivax malaria parasite. Proc Natl Acad Sci U S A. 1993; 90(22):10793–10797. [PubMed: 8248172]
2. Neote K, Mak JY, Kolakowski LF Jr, Schall TJ. Functional and biochemical analysis of the cloned Duffy antigen: identity with the red blood cell chemokine receptor. Blood. 1994; 84(1):44–52. [PubMed: 7517217]
3. Chaudhuri A, Zbrzezna V, Polyakova J, Pogo AO, Hesselgesser J, Horuk R. Expression of the Duffy antigen in K562 cells. Evidence that it is the human erythrocyte chemokine receptor. J Biol Chem. 1994; 269(11):7835–7838. [PubMed: 8132497]
4. Gardner L, Patterson AM, Ashton BA, Stone MA, Middleton J. The human Duffy antigen binds selected inflammatory but not homeostatic chemokines. Biochem Biophys Res Commun. 2004; 321(2):306–312. [PubMed: 15358176]
5. Cancellieri C, Vacchini A, Locati M, Bonecchi R, Borroni EM. Atypical chemokine receptors: from silence to sound. Biochem Soc Trans. 2013; 41(1):231–236. [PubMed: 23356288]
6. Cutbush M, Mollison PL. The Duffy blood group system. Heredity (Edinb). 1950; 4(3):383–389. [PubMed: 14802995]
7. Cutbush M, Mollison PL, Parkin DM. A New Human Blood Group. Nature. 1950; 165(188–189)

8. Dawson TC, Lentsch AB, Wang Z, Cowhig JE, Rot A, Maeda N, Peiper SC. Exaggerated response to endotoxin in mice lacking the Duffy antigen/receptor for chemokines (DARC). Blood. 2000; 96(5):1681–1684. [PubMed: 10961863]

9. Lee JS, Wurfel MM, Matute-Bello G, Frevert CW, Rosengart MR, Ranganathan M, Wong VW, Holden T, Sutlief S, Richmond A, et al. The Duffy antigen modifies systemic and local tissue chemokine responses following lipopolysaccharide stimulation. J Immunol. 2006; 177(11):8086–8094. [PubMed: 17114483]

10. Tournamille C, Colin Y, Cartron JP, Le Van Kim C. Disruption of a GATA motif in the Duffy gene promoter abolishes erythroid gene expression in Duffy-negative individuals. Nat Genet. 1995; 10(2):224–228. [PubMed: 7663520]

11. Miller LH, Mason SJ, Clyde DF, McGinniss MH. The resistance factor to Plasmodium vivax in blacks. The Duffy-blood-group genotype, FyFy. N Engl J Med. 1976; 295(6):302–304. [PubMed: 778616]

12. Hadley TJ, Lu ZH, Wasniowska K, Martin AW, Peiper SC, Hesselgesser J, Horuk R. Postcapillary venule endothelial cells in kidney express a multispecific chemokine receptor that is structurally and functionally identical to the erythroid isoform, which is the Duffy blood group antigen. J Clin Invest. 1994; 94(3):985–991. [PubMed: 8083383]

13. Pruenster M, Mudde L, Bombosi P, Dimitrova S, Zsak M, Middleton J, Richmond A, Graham GJ, Segerer S, Nibbs RJ, et al. The Duffy antigen receptor for chemokines transports chemokines and supports their promigratory activity. Nat Immunol. 2009; 10(1):101–108. [PubMed: 19060902]

14. Horuk R, Martin A, Hesselgesser J, Hadley T, Lu ZH, Wang ZX, Peiper SC. The Duffy antigen receptor for chemokines: structural analysis and expression in the brain. J Leukoc Biol. 1996; 59(1):29–38. [PubMed: 8558064]

15. Horuk R, Martin AW, Wang Z, Schweitzer L, Gerassimides A, Guo H, Lu Z, Hesselgesser J, Perez HD, Kim J, et al. Expression of chemokine receptors by subsets of neurons in the central nervous system. J Immunol. 1997; 158(6):2882–2890. [PubMed: 9058825]

16. Lein ES, Hawrylycz MJ, Ao N, Ayres M, Bensinger A, Bernard A, Boe AF, Boguski MS, Brockway KS, Byrnes EJ, et al. Genome-wide atlas of gene expression in the adult mouse brain. Nature. 2007; 445(7124):168–176. [PubMed: 17151600]

17. Luo H, Chaudhuri A, Johnson KR, Neote K, Zbrzezna V, He Y, Pogo AO. Cloning, characterization, and mapping of a murine promiscuous chemokine receptor gene: homolog of the human Duffy gene. Genome Res. 1997; 7(9):932–941. [PubMed: 9314499]

18. van Gassen KL, Netzeband JG, de Graan PN, Gruol DL. The chemokine CCL2 modulates Ca2+ dynamics and electrophysiological properties of cultured cerebellar Purkinje neurons. Eur J Neurosci. 2005; 21(11):2949–2957. [PubMed: 15978006]

19. Giovannelli A, Limatola C, Ragozzino D, Mileo AM, Ruggieri A, Ciotti MT, Mercanti D, Santoni A, Eusebi F. CXC chemokines interleukin-8 (IL-8) and growth-related gene product alpha (GROalpha) modulate Purkinje neuron activity in mouse cerebellum. J Neuroimmunol. 1998; 92(1–2):122–132. [PubMed: 9916887]

20. Lentsch AB. The Duffy antigen/receptor for chemokines (DARC) and prostate cancer. A role as clear as black and white? Faseb J. 2002; 16(9):1093–1095. [PubMed: 12087071]

21. Mei J, Liu Y, Dai N, Favara M, Greene T, Jeyaseelan S, Poncz M, Lee JS, Worthen GS. CXCL5 regulates chemokine scavenging and pulmonary host defense to bacterial infection. Immunity. 2010; 33(1):106–117. [PubMed: 20643340]

22. Ragozzino D, Giovannelli A, Mileo AM, Limatola C, Santoni A, Eusebi F. Modulation of the neurotransmitter release in rat cerebellar neurons by GRO beta. Neuroreport. 1998; 9(16):3601–3606. [PubMed: 9858367]

23. Gillard SE, Lu M, Mastracci RM, Miller RJ. Expression of functional chemokine receptors by rat cerebellar neurons. J Neuroimmunol. 2002; 124(1–2):16–28. [PubMed: 11958818]

24. Luo H, Chaudhuri A, Zbrzezna V, He Y, Pogo AO. Deletion of the murine Duffy gene (Dfy) reveals that the Duffy receptor is functionally redundant. Mol Cell Biol. 2000; 20(9):3097–3101. [PubMed: 10757794]

25. Rios M, Chaudhuri A, Mallinson G, Sausais L, Gomensoro-Garcia AE, Hannon J, Rosenberger S, Poole J, Burgess G, Pogo O, et al. New genotypes in Fy(a-b-) individuals: nonsense mutations

(Trp to stop) in the coding sequence of either FY A or FY B. Br J Haematol. 2000; 108(2):448–454. [PubMed: 10691880]

26. Lalonde R, Filali M, Bensoula AN, Lestienne F. Sensorimotor learning in three cerebellar mutant mice. Neurobiol Learn Mem. 1996; 65(2):113–120. [PubMed: 8833100]
27. Lalonde R, Botez MI, Joyal CC, Caumartin M. Motor abnormalities in lurcher mutant mice. Physiol Behav. 1992; 51(3):523–525. [PubMed: 1523229]
28. Lalonde R, Strazielle C. Motor coordination, exploration, and spatial learning in a natural mouse mutation (nervous) with Purkinje cell degeneration. Behav Genet. 2003; 33(1):59–66. [PubMed: 12645822]
29. Baldacara L, Borgio JG, Lacerda AL, Jackowski AP. Cerebellum and psychiatric disorders. Rev Bras Psiquiatr. 2008; 30(3):281–289. [PubMed: 18833430]
30. Hilber P, Lorivel T, Delarue C, Caston J. Stress and anxious-related behaviors in Lurcher mutant mice. Brain Res. 2004; 1003(1–2):108–112. [PubMed: 15019569]
31. Handforth A. Harmaline tremor: underlying mechanisms in a potential animal model of essential tremor. Tremor Other Hyperkinet Mov (N Y). 2012; 2 http://tremorjournal.org/article/view/92(.
32. D'Hooge R, De Deyn PP. Applications of the Morris water maze in the study of learning and memory. Brain Res Brain Res Rev. 2001; 36(1):60–90. [PubMed: 11516773]
33. Lalonde R, Strazielle C. The effects of cerebellar damage on maze learning in animals. Cerebellum. 2003; 2(4):300–309. [PubMed: 14964689]
34. Crawley, JN. What's Wrong With My Mouse? - Behavioral Phenotyping of Transgenic and Knockout Mice. Hoboken, New Jersey: John Wiley & Sons, Inc; 2007.
35. Trivedi R, Khan AR, Rana P, Haridas S, Hemanth Kumar BS, Manda K, Rathore RK, Tripathi RP, Khushu S. Radiation-induced early changes in the brain and behavior: serial diffusion tensor imaging and behavioral evaluation after graded doses of radiation. J Neurosci Res. 2012; 90(10): 2009–2019. [PubMed: 22605562]
36. Fowler SC, Miller BR, Gaither TW, Johnson MA, Rebec GV. Force-plate quantification of progressive behavioral deficits in the R6/2 mouse model of Huntington's disease. Behav Brain Res. 2009; 202(1):130–137. [PubMed: 19447289]
37. Fowler SC, Zarcone TJ, Vorontsova E, Chen R. Motor and associative deficits in D2 dopamine receptor knockout mice. Int J Dev Neurosci. 2002; 20(3–5):309–321. [PubMed: 12175868]
38. Aspide R, Gironi Carnevale UA, Sergeant JA, Sadile AG. Non-selective attention and nitric oxide in putative animal models of Attention-Deficit Hyperactivity Disorder. Behav Brain Res. 1998; 95(1):123–133. [PubMed: 9754884]
39. Chaumont J, Guyon N, Valera AM, Dugue GP, Popa D, Marcaggi P, Gautheron V, Reibel-Foisset S, Dieudonne S, Stephan A, et al. Clusters of cerebellar Purkinje cells control their afferent climbing fiber discharge. Proc Natl Acad Sci U S A. 2013
40. Milner TE, Cadoret G, Lessard L, Smith AM. EMG analysis of harmaline-induced tremor in normal and three strains of mutant mice with Purkinje cell degeneration and the role of the inferior olive. J Neurophysiol. 1995; 73(6):2568–2577. [PubMed: 7666163]
41. Peiper SC, Wang ZX, Neote K, Martin AW, Showell HJ, Conklyn MJ, Ogborne K, Hadley TJ, Lu ZH, Hesselgesser J, et al. The Duffy antigen/receptor for chemokines (DARC) is expressed in endothelial cells of Duffy negative individuals who lack the erythrocyte receptor. J Exp Med. 1995; 181(4):1311–1317. [PubMed: 7699323]
42. Lalonde R, Botez MI, Boivin D. Spontaneous alternation and habituation in a t-maze in nervous mutant mice. Behav Neurosci. 1986; 100(3):350–352. [PubMed: 3730141]
43. Dickson PE, Rogers TD, Del Mar N, Martin LA, Heck D, Blaha CD, Goldowitz D, Mittleman G. Behavioral flexibility in a mouse model of developmental cerebellar Purkinje cell loss. Neurobiol Learn Mem. 2010; 94(2):220–228. [PubMed: 20566377]
44. Korelusova I, Cendelin J, Vozez F. Motor and visuospatial abilities in a model of olivocerebellar and retinal degeneration--Lurcher mutant mice of C3H strain. Prague Med Rep. 2007; 108(1):37–48.
45. Baltanas FC, Casafont I, Lafarga V, Weruaga E, Alonso JR, Berciano MT, Lafarga M. Purkinje cell degeneration in pcd mice reveals large scale chromatin reorganization and gene silencing linked to defective DNA repair. J Biol Chem. 2011; 286(32):28287–28302. [PubMed: 21700704]

46. Banisadr G, Gosselin RD, Mechighel P, Kitabgi P, Rostene W, Parsadaniantz SM. Highly regionalized neuronal expression of monocyte chemoattractant protein-1 (MCP-1/CCL2) in rat brain: evidence for its colocalization with neurotransmitters and neuropeptides. J Comp Neurol. 2005; 489(3):275–292. [PubMed: 16025454]

47. Florenzano F, Bentivoglio M. Degranulation, density, and distribution of mast cells in the rat thalamus: a light and electron microscopic study in basal conditions and after intracerebroventricular administration of nerve growth factor. J Comp Neurol. 2000; 424(4):651–669. [PubMed: 10931487]

48. Marshall JS. Mast-cell responses to pathogens. Nat Rev Immunol. 2004; 4(10):787–799. [PubMed: 15459670]

49. Nautiyal KM, Ribeiro AC, Pfaff DW, Silver R. Brain mast cells link the immune system to anxiety-like behavior. Proc Natl Acad Sci U S A. 2008; 105(46):18053–18057. [PubMed: 19004805]

50. Ambrosini E, Aloisi F. Chemokines and glial cells: a complex network in the central nervous system. Neurochem Res. 2004; 29(5):1017–1038. [PubMed: 15139300]

51. Chakera A, Seeber RM, John AE, Eidne KA, Greaves DR. The duffy antigen/receptor for chemokines exists in an oligomeric form in living cells and functionally antagonizes CCR5 signaling through hetero-oligomerization. Mol Pharmacol. 2008; 73(5):1362–1370. [PubMed: 18230715]

52. Adler MW, Geller EB, Chen X, Rogers TJ. Viewing chemokines as a third major system of communication in the brain. Aaps J. 2005; 7(4):E865–E870. [PubMed: 16594639]

53. Fowler SC, Birkestrand BR, Chen R, Moss SJ, Vorontsova E, Wang G, Zarcone TJ. A force-plate actometer for quantitating rodent behaviors: illustrative data on locomotion, rotation, spatial patterning, stereotypies, and tremor. J Neurosci Methods. 2001; 107(1–2):107–124. [PubMed: 11389948]

54. Lalonde R, Lamarre Y, Smith AM, Botez MI. Spontaneous alternation and habituation in lurcher mutant mice. Brain Res. 1986; 362(1):161–164. [PubMed: 3942864]

55. Lalonde R, Thifault S. Absence of an association between motor coordination and spatial orientation in lurcher mutant mice. Behav Genet. 1994; 24(6):497–501. [PubMed: 7872930]

56. Lalonde R, Manseau M, Botez MI. Spontaneous alternation and habituation in Purkinje cell degeneration mutant mice. Brain Res. 1987; 411(1):187–189. [PubMed: 3607423]

57. Goodlett CR, Hamre KM, West JR. Dissociation of spatial navigation and visual guidance performance in Purkinje cell degeneration (pcd) mutant mice. Behav Brain Res. 1992; 47(2):129–141. [PubMed: 1590945]

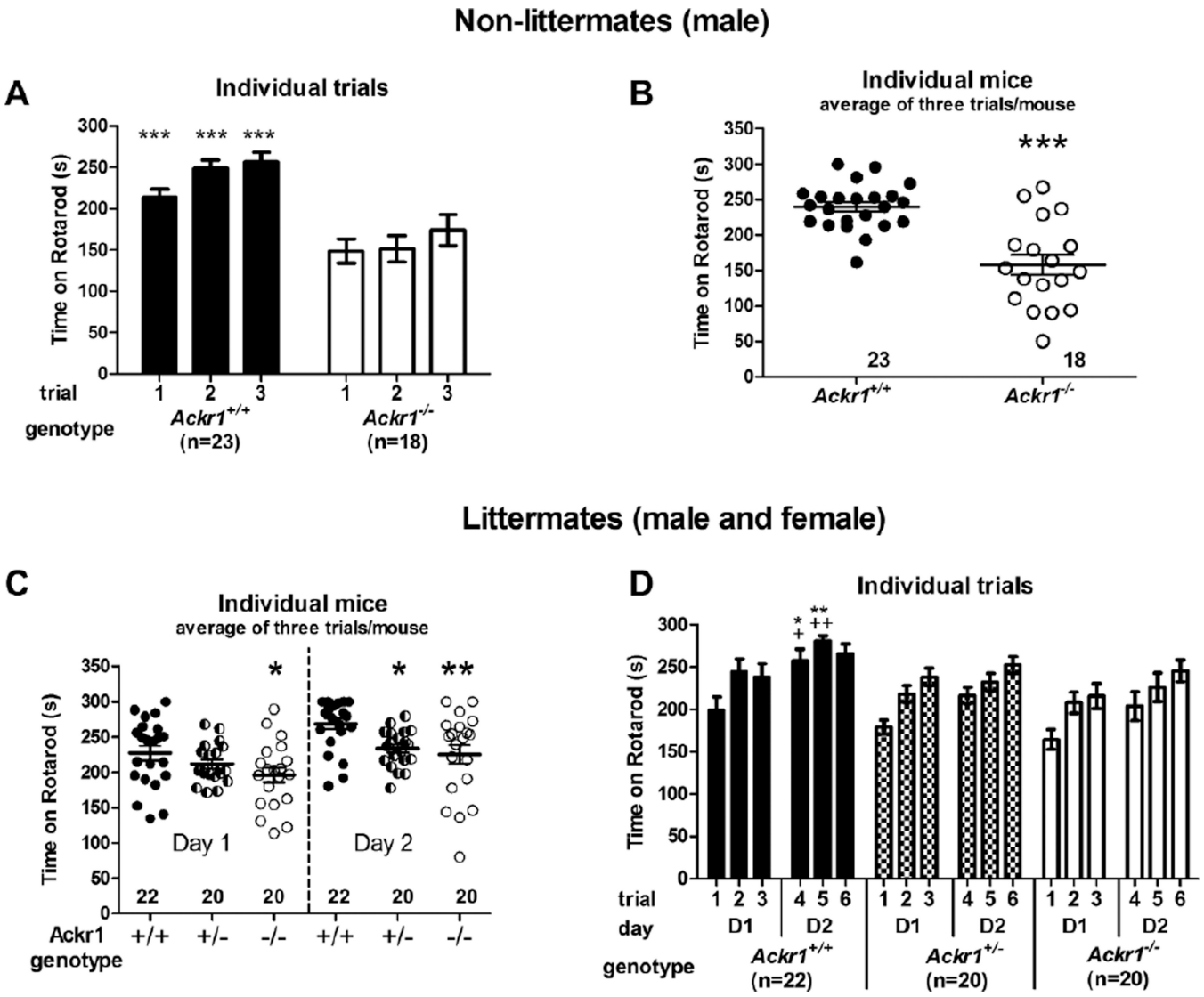

Figure 1.

Ackr1 deficiency impairs balance on a rotating rod (rotarod). (A, B) Male non-littermate *Ackr1*$^{+/+}$ and *Ackr1*$^{-/-}$ mice. (A) Rotarod performance in three consecutive trials performed on the same day. (B) Rotarod performance of individual mice, average of all three trials per mouse. (C, D) Littermate *Ackr1*$^{+/+}$*Ackr1*$^{+/-}$ and *Ackr1*$^{-/-}$ mice (data for male and female mice merged). (C) Rotarod performance of the individual mice, average of all three trials per mouse and day. (D) Rotarod performance in six individual trials performed on two consecutive experimental days (three trials per day). Data shown are means ± SEM; the number of animals is given in the figures. *Ackr1*$^{-/-}$ mice and *Ackr1*$^{+/-}$ animals were compared with *Ackr1*$^{+/+}$ controls by t-test (A, B) or 1-way ANOVA and Newman-Keuls post-test (C). In (D), all three groups of mice were compared for each trial by 1-way ANOVA and Newman-Keuls post-test with *: comparison *Ackr1*$^{+/+}$ to *Ackr1*$^{-/-}$ and +: comparison *Ackr1*$^{+/+}$ to *Ackr1*$^{+/-}$. One symbol: $p<0.05$; two symbols: $p<0.005$; three symbols: $p<0.001$.

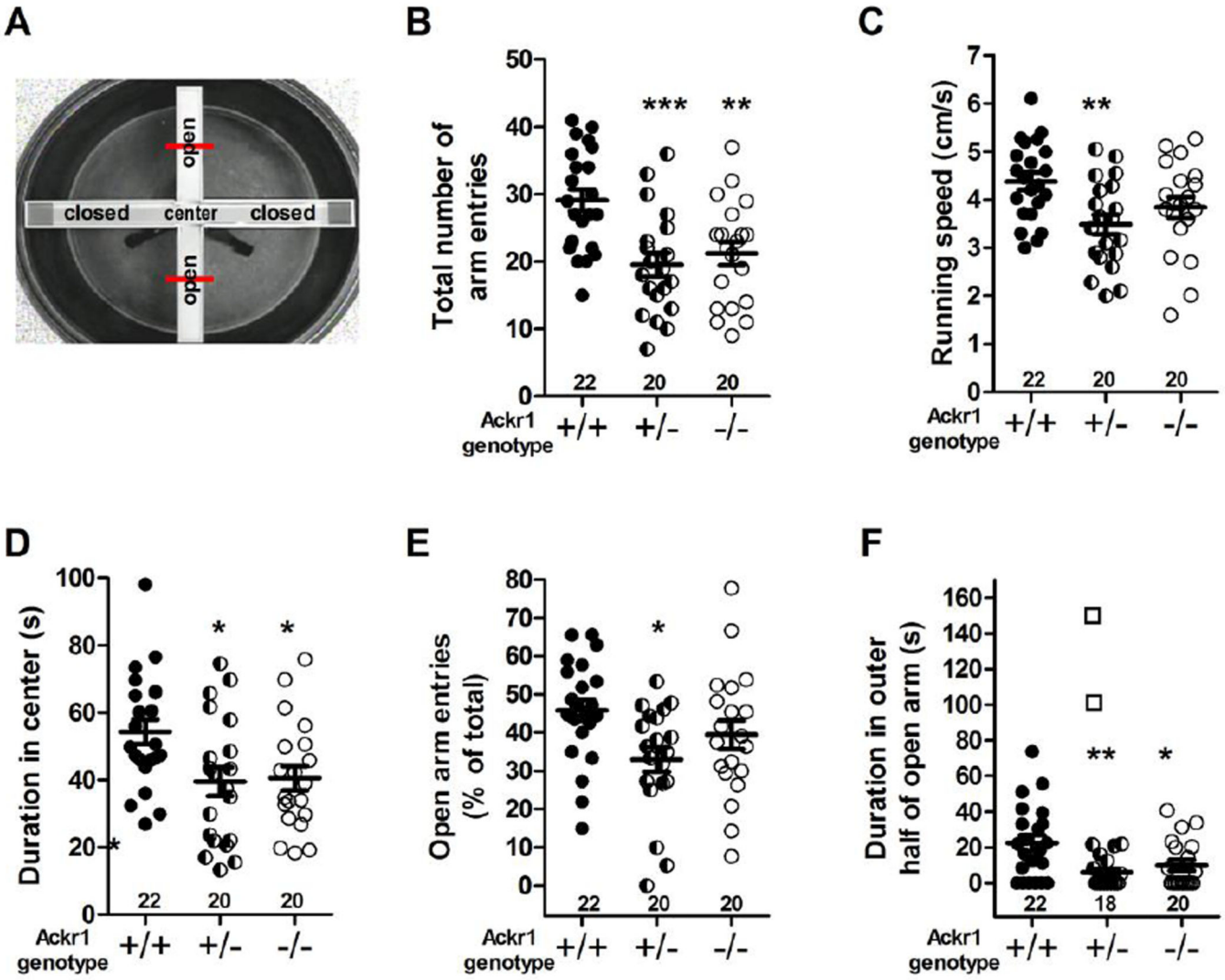

Figure 2.

Ackr1 deficiency impairs locomotion and promotes anxiety-like behavior on the elevated plus maze. (A) Elevated plus maze experimental setup. The red lines indicate the threshold that defines “open arm end”. (B) Total number of arm entries. (C) Average running speed in cm/s. (D) Duration of time spent in the center square of the elevated plus maze. (E) Percentage of open arm entries, related to total number of arm entries. (F) Time spent in open arm end (open squares: two outliers that were excluded from analysis). Data shown are means ± SEM; the number of animals is given in the figures. *Ackr1*$^{-/-}$ mice and heterozygous animals were compared with C57Bl/6 controls by 1-way ANOVA and Newman-Keuls post-test; * $p<0.05$; ** $p<0.005$; *** $p<0.001$.

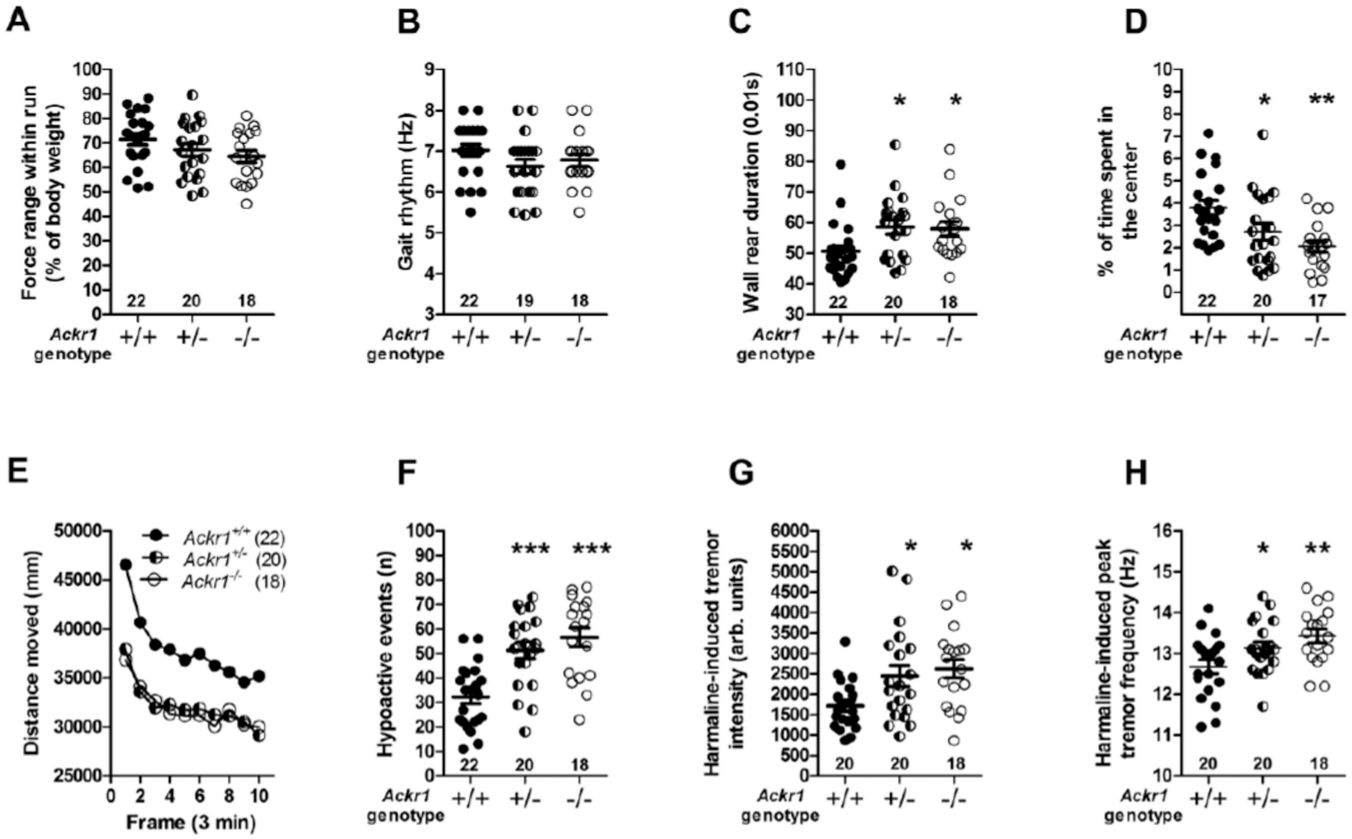

Figure 3.

Ackr1 deficiency impairs spontaneous locomotion but induces spontaneous anxiety like-behavior and worsens harmaline-induced cerebellar tremor. All data were obtained during 30 minute sessions on a force plate actometer after injection of either PBS (A–F) or harmaline (G, H). (A) Range of force variations produced during long run sequences; (B) Gait rhythm during long runs; (C) Duration of wall rears; (D) Percentage of time spent in the center of the force plate; (E) Locomotor activity (distance moved in 3 min time frames); (F) Number of hypoactive events (Time periods >5 s with the animal moving in a radius of < 15 mm); (G) Intensity of harmaline-induced tremor; (H) Frequency of Harmaline-induced tremor. Data shown are means ± SEM. (A, B, C, D, F, G, H) Comparison of $Ackr1^{+/-}$ and $Ackr1^{-/-}$ mice with $Ackr1^{+/+}$ controls, 1-way ANOVA with Newman-Keuls post-test; * $p<0.05$; ** $p<0.005$; *** $p<0.001$; (E) Comparison of the curves with 2-way ANOVA ($p = 0.002$ for $Ackr1^{+/+}$ *vs*. $Ackr1^{+/-}$ and $p = 0.005$ for comparison $Ackr1^{+/+}$ *vs*. $Ackr1^{-/-}$). SEM in (E) is < 6% of the mean for each point.

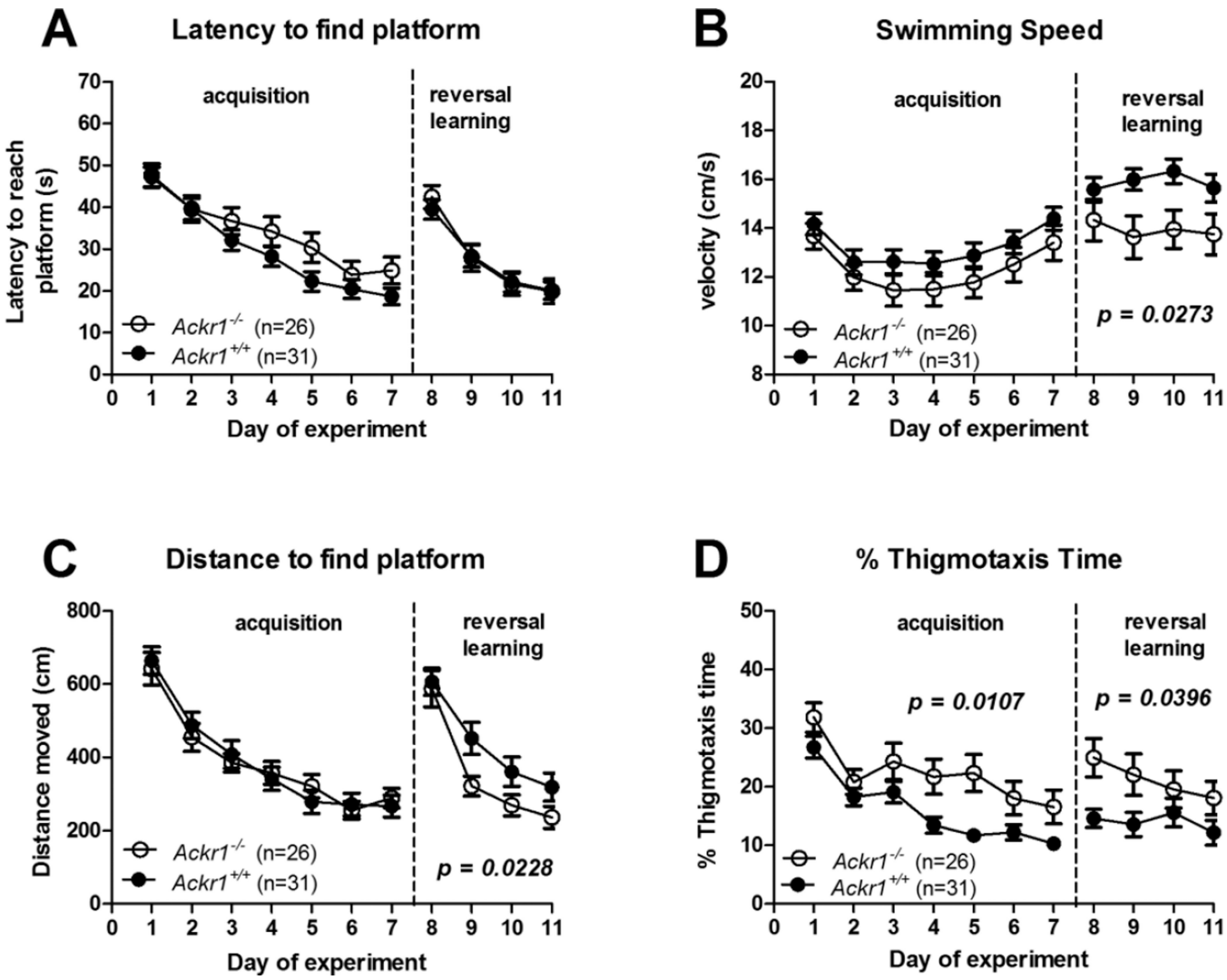

Figure 4.

Characterization of spatial learning of *Ackr1*$^{+/+}$ and *Ackr1*$^{-/-}$ mice in the Morris water maze. (A) Latency to find the platform; (B) swimming speed; (C) swimming distance covered until the platform is found and (D) thigmotaxis time (time spent close to the edge of the water maze). Curves were compared by 2-way ANOVA with separate analyses for acquisition- and reversal learning phase. Summary data for all animals tested are presented as the mean +/− SEM. P-values are given in the graphs.

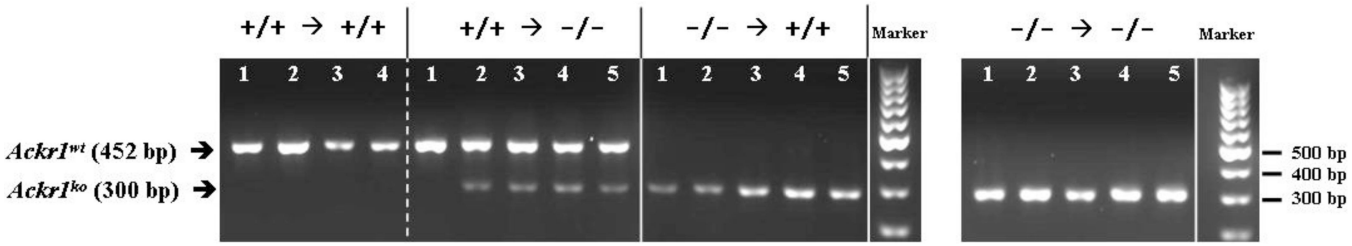

Figure 5.

Determination of bone marrow engraftment in radiation chimeras. Blood DNA was amplified by PCR, and amplicon size was determined by agarose gel electrophoresis. *Ackr1*^{wt} and *Ackr1*^{ko} amplicon positions are identified by arrows at the left side of the figure. Each group of samples represents chimeric mice of the same composition, which is indicated at the top of the panel coded as donor genotype ➔ recipient genotype. Left and right part of the figure each show an individual gel. Dashed lines separate groups of samples on a contiguous part of the gel, while straight lines indicate disconnected parts of the same gel. The numbers above the lanes in each panel represent chimerism in individual mouse replicates for each condition.

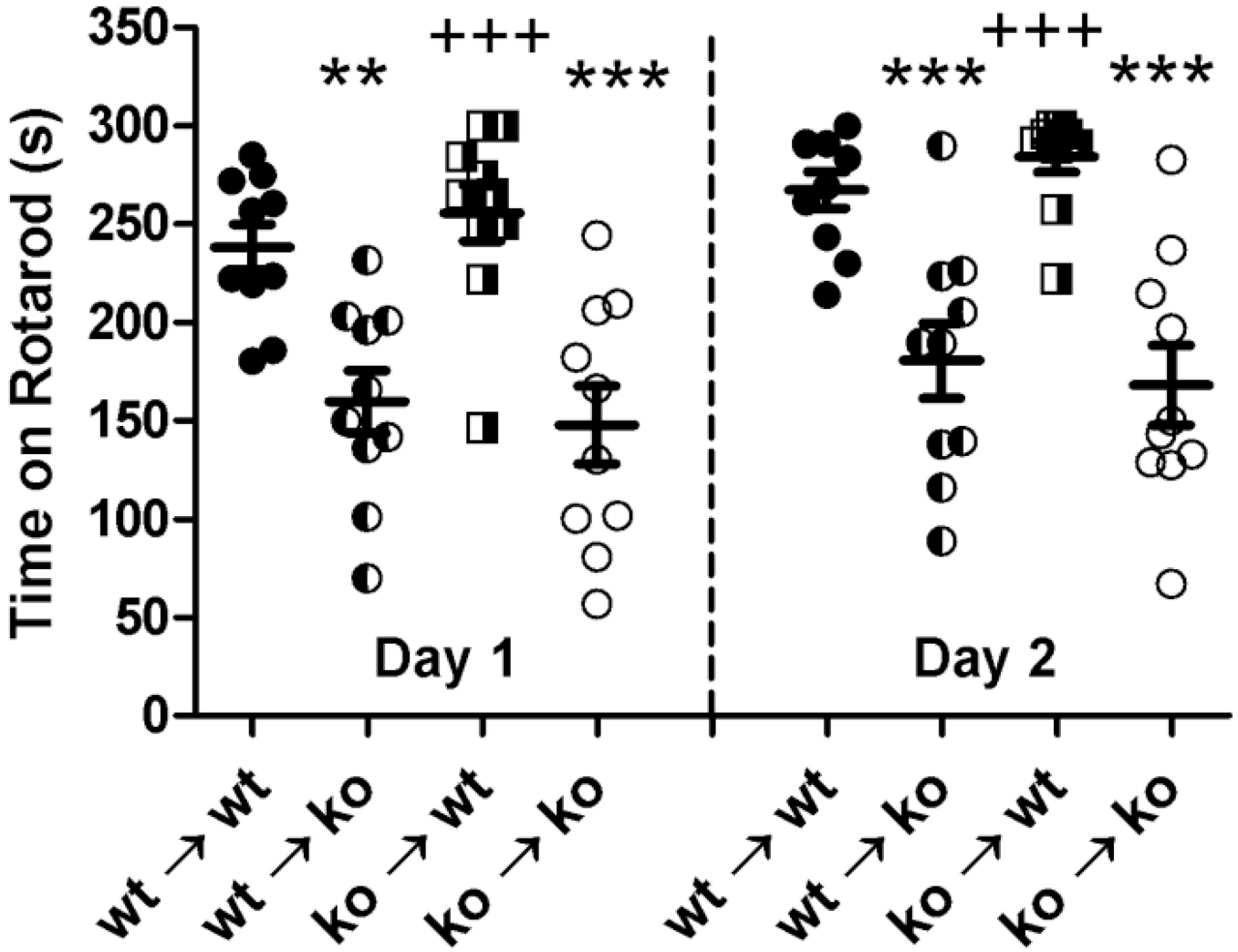

Figure 6.

Rotarod performance of radiation bone marrow chimeras (male and female mice). Mice were tested on two consecutive days with three trials perday per animal. The groups are shown below the x-axis (donor ➔ recipient). Each symbol represents a single mouse. Bars represent means ± SEM of the average times spent on the rotarod during three independent trials for each mouse on each day; the same mice were tested on day 1 and day 2; n=10 mice for each condition. Groups were compared by 1-way ANOVA with Newman-Keuls post test; * indicates significance in comparison to the *Ackr1*$^{+/+}$➔*Ackr1*$^{+/+}$ group; + indicates a significant difference to *Ackr1*$^{-/-}$➔*Ackr1*$^{-/-}$; one symbol: $p<0.05$; two symbols: $p<0.005$; three symbols: $p<0.001$.

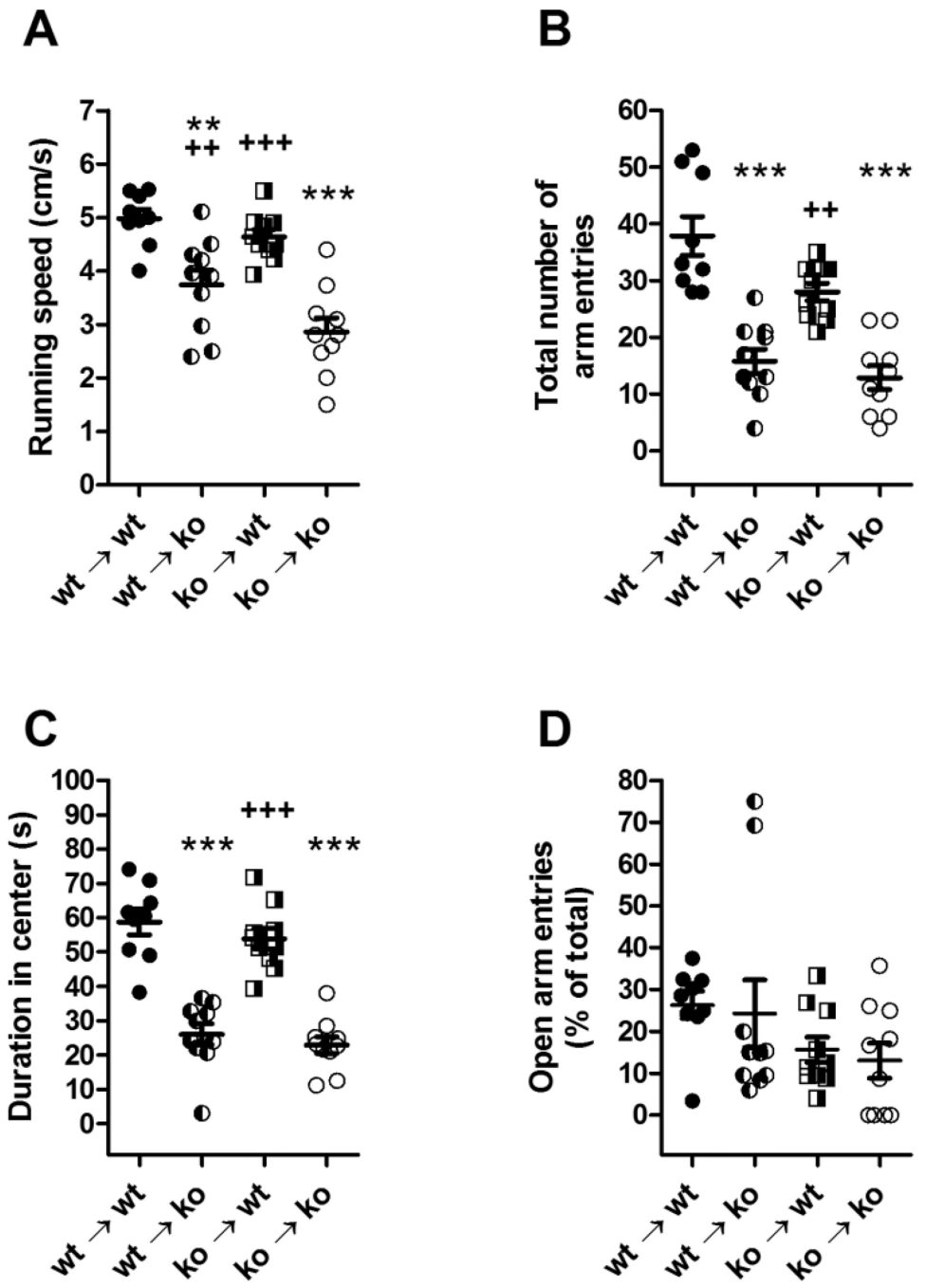

Figure 7.

Behavior of irradiation bone marrow chimeras on the elevated plus maze. (A) Average running speed, (B) total number of arm entries, (C) duration in center and (D) percentage of open arm entries. The groups are shown below the x-axis (donor ➔ recipient). Data shown are means ± SEM; each symbol represents a single mouse. Groups were compared by 1-way ANOVA with Newman-Keuls post test; * indicates significance in comparison to the *Ackr1*$^{+/+}$➔*Ackr1*$^{+/+}$ group; + indicates a significant difference compared to

Ackr1$^{-/-}$➔*Ackr1*$^{-/-}$; one symbol: $p<0.05$; two symbols: $p<0.005$; three symbols: $p<0.001$; n = 9–10 mice for each condition.

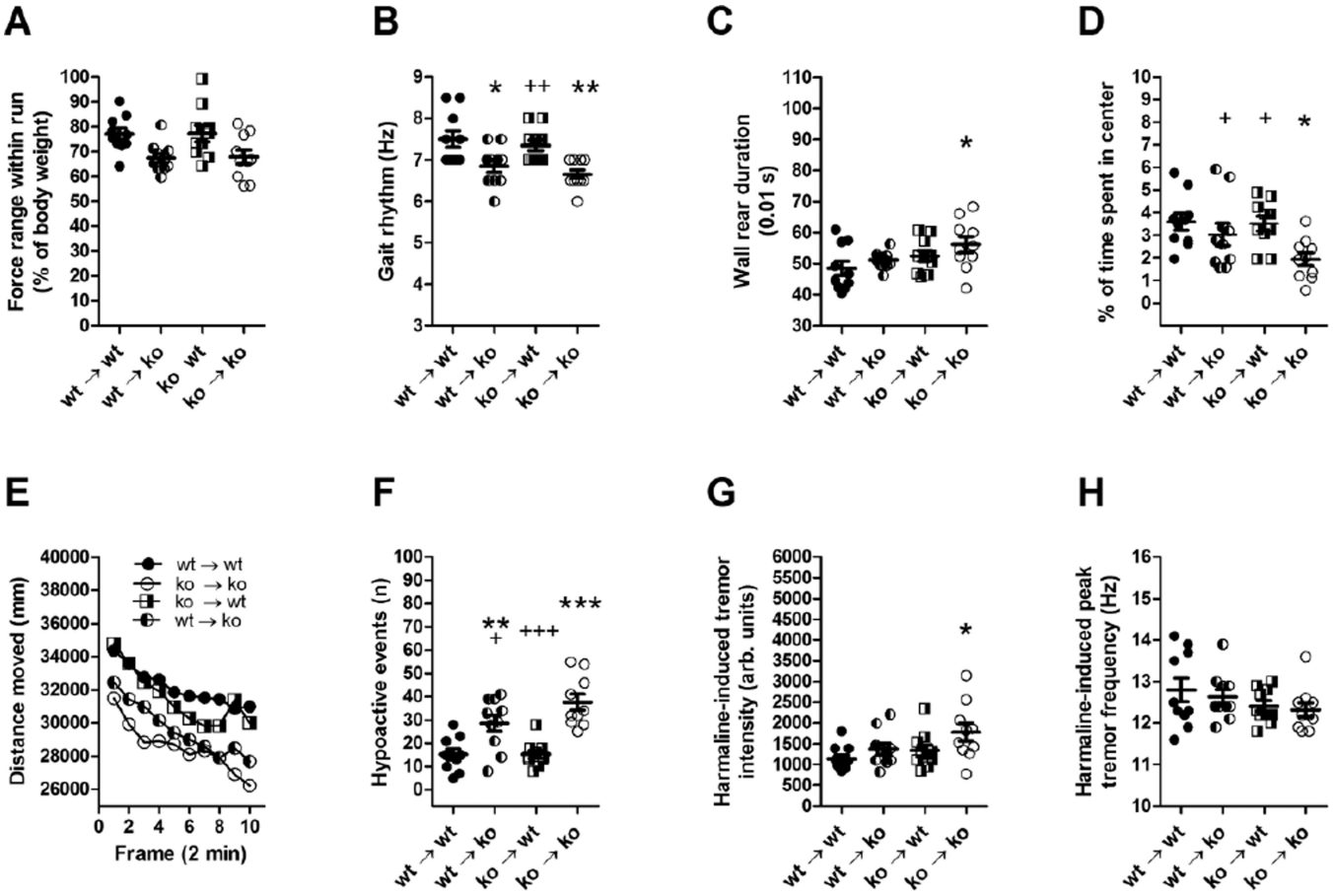

Figure 8.

Spontaneous behavior of radiation bone marrow chimeras on the force plate actometer. (A–F) 20 min sessions, starting 10 min after PBS injection; (G, H) 20 min sessions, starting 10 min after harmaline injection. (A) Range of force variations produced during long running sequences; (B) Gait rhythm during long runs; (C) Duration of wall rears; (D) Percentage of time spent in the center of the force plate; (E) Locomotor activity (distance moved in 2 min time frames); (F) Number of hypoactive events (Time periods >5 s with the animal moving in a radius of < 15 mm); (G) Intensity of harmaline-induced tremor; (H) Frequency of harmaline-induced tremor. Data shown are means ± SEM; n=10 mice for each condition. (A, B, C, D, F, G, H) Comparison of the groups by 1-way ANOVA with Newman-Keuls post test; * indicates significance in comparison to the *Ackr1*$^{+/+}$ ➔ *Ackr1*$^{+/+}$; + indicates a significant difference to *Ackr1*$^{-/-}$ ➔ *Ackr1*$^{-/-}$; one symbol: $p<0.05$; two symbols: $p<0.005$; three symbols: $p<0.001$; (E) Comparison of the curves with 2-way ANOVA (significant differences: $p = 0.011$ for *Ackr1*$^{+/+}$➔*Ackr1*$^{+/+}$ *vs.* *Ackr1*$^{-/-}$➔*Ackr1*$^{-/-}$ and $p = 0.030$ for *Ackr1*$^{-/-}$➔*Ackr1*$^{-/-}$*vs.* *Ackr1*$^{-/-}$➔*Ackr1*$^{+/+}$). SEM in (E) is < 5% of the mean for each point.

Table 1

Average number of 180° turns per minute on the rotarod beam for the littermate experiments

	Ackr1$^{+/+}$ turns/min	**Ackr1$^{+/-}$ turns/min**	**Ackr1$^{-/-}$ turns/min**
Day 1	0.89 ± 0.18 (n=22)	0.48 ± 0.14 (n=20)	0.40 ± 0.13* (n=20)
Day 2	0.61 ± 0.13 (n=21)	0.33 ± 0.10 (n=20)	0.57 ± 0.20 (n=19)

* $p < 0.05$, compared to Ackr1$^{+/+}$ (Mann-Whitney *U* test)

Table 2

Behavior of mice with cerebellar degeneration – comparison to *Ackr1*$^{-/-}$ animals

Mouse strain	Harmaline tremor intensity[1]	harmaline tremor frequency[1]	locomotor activity	reverse learning, behavioral flexibility	water maze acquisition learning[5]	anxiety	rotarod per-formance
Lurcher (lc/+)	no tremor observed (40)		unchanged[3] (54)	impaired[4] (43)	impaired (55)	reduced[6] (30)	impaired (44)
Lurcher (lc/+ ↔ +/+) Aggregation chimeras	n.d.		n.d.	impaired[4] (43)	n.d.	n.d.	n.d.
Purkinje cell Degeneration (pcd/pcd)	reduced[1] unchanged[2] (40)	reduced[1,2] (40)	unchanged[3] (56)	n.d.	impaired (57)	n.d.	impaired (45)
nervous (nr/nr)	reduced[1,2] (40)	reduced[1,2] (40)	increased (28, 42)[3]	n.d.	impaired (28)	n.d.	impaired (28)
Ackr1$^{-/-}$	increased	increased	reduced	improved	unchanged	increased	impaired

[1] electromyogram;

[2] platform-mounted accelerometer;

[3] T-maze; activity in ref.(42) showed a non-significant trend;

[4] operant conditional visual discrimination with 4 reversals;

[5] parameter: reduction of path length to find platform;

[6] interpreted as reduced behavioral inhibition

n.d. = not determined, no literature report was found

Behav Genet. Author manuscript; available in PMC 2016 March 14.